

## Reflectivity and Optical Brightness of Laser-Induced Shocks in Silicon

Th. Löwer, V. N. Kondrashov,\* M. Basko,† A. Kendl, J. Meyer-ter-Vehn, and R. Sigel‡

*Max-Planck-Institut für Quantenoptik, D-85748 Garching, Germany*

A. Ng

*Department of Physics and Astronomy, The University of British Columbia, Vancouver, British Columbia, V6T 1Z1, Canada*

(Received 23 April 1997; revised manuscript received 5 January 1998)

We report the first simultaneous measurement of the reflectivity and optical emission of a strong (4–8 Mbar) shock front emerging at a free surface of a solid. Planar shock waves were driven by thermal x rays from a laser-heated cavity. The inferred model-independent brightness temperature of the shock front in silicon turns out to be significantly below the expected Hugoniot temperature. We find that our data cannot be explained within the two-temperature model which assumes instantaneous metallization of silicon in the density jump. [S0031-9007(98)06017-7]

PACS numbers: 71.30.th, 52.35.Tc, 62.50.+p, 78.20.Ci

Direct optical measurements of the Hugoniot temperatures in matter compressed by strong shock waves could provide extremely valuable information about the equation of state (EOS) at high pressures [1], which has a wide range of applications from astrophysics to controlled fusion research. Corresponding experiments require (i) high-quality planar shock waves driven without preheat parallel to the sample surface, (ii) sufficiently high temporal resolution, and (iii) simultaneous measurement of the reflectivity and absolute emission of the emerging shock front to infer its brightness temperature. Also, the shocked material must be in a metallic state because otherwise a long relaxation zone (discovered earlier in ionic crystals [2]) obscures the postshock equilibrium state. In this Letter we report the results of an experiment where all of these conditions have for the first time been met in silicon.

As was first realized by Celliers *et al.* [3,4], silicon has an advantage of being semitransparent in its normal state and, with a band gap of only 1.1 eV, becomes metallic under static pressures above 0.2 Mbar [5]. The absorption coefficient of  $\sim 10^4 \text{ cm}^{-1}$  for the visible light in the unperturbed state ensures that the final approach to the free surface by a  $\sim 20 \text{ km/s}$  shock front can be resolved with modern streak cameras.

Important progress, as compared to Refs. [3,4], has been achieved in our paper (i) by employing indirect drive with a novel type of x-ray cavity [6,7] to launch planar preheat-free shock waves, and (ii) by augmenting the emission data with simultaneous measurements of the monochromatic reflectivity of the shock front. We believe that we have for the first time measured the reflectivity of a shock front in flight as it propagates in solid matter. Similar to cold metals, this quantity alone provides valuable information on the electron-ion (*e-i*) relaxation time in the shock compressed state. By applying Kirchhoff's law to the measured reflectivity and emission values, we obtain a *model-independent* estimate for the brightness temperature of the shock front, which turns out

to be significantly below the expected Hugoniot temperature. This confirms the earlier conclusion by Celliers *et al.* [3,4] that the shock emission is strongly affected by its nonequilibrium structure. However, all our efforts to reproduce the observed emission signals (which we believe to be superior to all previous measurements) within the conventional two-temperature (*2-T*) model [4,7,8] have essentially failed. We conclude that a new type of nonequilibrium model is needed to interpret pyrometric measurements of the shock fronts in semiconductors.

The experimental arrangement of the x-ray cavity ( $\varnothing = 1 \text{ mm}$ ) and the sample is shown at the top of Fig. 1. The gold cavity is heated by a single beam of the Asterix iodine laser emitting a 250 J, 450 ps,  $0.44 \mu\text{m}$  pulse. The laser light hits a gold converter cone at the center, which shields the sample against preheat by primary x rays from the laser produced plasma. The sample, positioned on the axis of the rotationally symmetric cavity, is made of polished (roughness below 0.5 nm) intrinsic silicon in thicknesses of 13–27  $\mu\text{m}$  and glued onto a 300  $\mu\text{m}$  hole in the cavity.

Optical emission and reflection are detected with a temporal resolution of 7 ps by imaging the sample onto the streak slit of a Hadland Imacon 500 streak camera with digital CCD readout, carefully operated in the linear range. As shown in Fig. 1, one-half of the sample is used to measure reflectivity with the help of a pulsed probe laser emitting at a wavelength of  $\lambda = 532 \text{ nm}$ . Self-emission is suppressed by a neutral-density 2.5% transmission filter, which covers the probe-laser irradiated part of the sample and is fixed on the streak slit (i.e., in the image plane). The registered emission signal is received from the other half of the sample. In addition, a probe-laser fiducial and an Asterix laser fiducial are generated by using optical fibers. The whole setup was absolutely calibrated *in situ* by switching over to the spectrograph mode of the streak camera and using the 532 nm probe laser to simulate the emission of the sample (for more

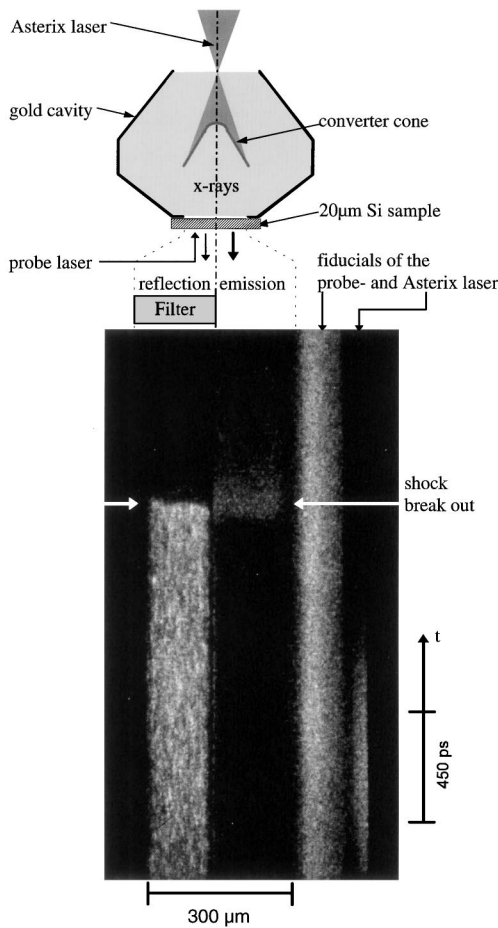


FIG. 1. Top: laser heated driver cavity, sample and setup for detection of optical signals (schematic). Bottom: streak image showing spatially resolved traces of reflected probe-laser light and sample emission together with two laser fiducials. The Asterix fiducial signal is delayed by 560 ps with respect to the main pulse to appear in the camera time window.

details, see Ref. [7]. The shock speed was determined by using step targets. The typical shock speeds in our experiments were 17–22 km/s. This corresponds to shock pressures of 4–8 Mbar in silicon.

The streak image in Fig. 1 shows the temporal and spatial evolution of reflection and emission across the sample. The drop to zero in the reflected light and simultaneous rise of emission indicate shock arrival at the free surface. The emission then decays rapidly as the shock heated material expands and cools. Synchronism of the events along the streak slit, indicating the arrival of a planar shock parallel to the surface, was found to depend critically on careful alignment of the cavity and the heating laser beam, and on the quality and cleanness of the samples.

Figure 2 shows how the emission signal, measured in two spectral bands  $\lambda = 400\text{--}500\text{ nm}$  and  $\lambda = 570\text{--}630\text{ nm}$ , rises as the shock front of 22.5 km/s approaches the silicon surface. A dynamic range of a factor of 200 was achieved by covering one-half of the

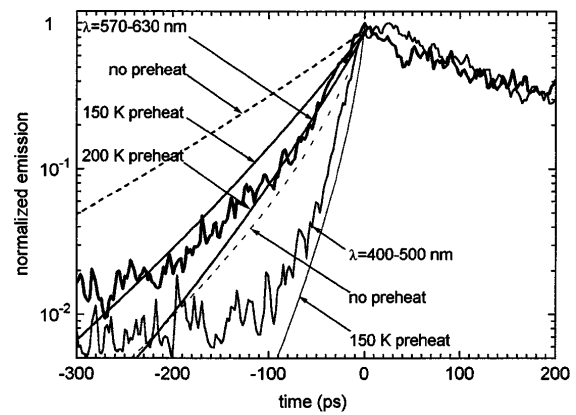


FIG. 2. Rise of optical emission signals (normalized to their peak values) in two spectral bands together with predictions for the indicated levels of preheat.

sample with a neutral-density 25% transmission filter. Comparing these measurements (noisy curves) with the signals calculated for a 1.4 eV Planckian source by using the known temperature and frequency dependences of the silicon absorption coefficient [9] and the spectral sensitivity of our color filters and photocathode (smooth dashed and solid curves), we conclude that the preheat in our experiments was not higher than 150–200 K.

The streak image in Fig. 1 was taken with a bare (uncoated) silicon sample. The corresponding traces for the reflected and emitted signals (both at  $\lambda = 532\text{ nm}$ ) are plotted in Fig. 3. Because of the high index of refraction,  $n = 4.15$ , the silicon surface reflects a constant fraction of 37% of the probe light (the observed fluctuations being attributed to probe-laser speckles), making discrimination of a comparable or lower reflectivity of the shock front virtually impossible. To obtain unambiguous data for the latter, we performed experiments with silicon samples coated with a 70 nm antireflection (AR) layer of  $\text{Si}_3\text{N}_4$  ( $n = 2.01$ ). Distortions of optical signals due to shock

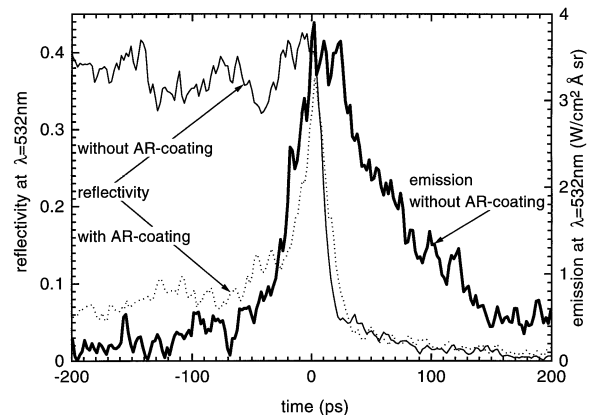


FIG. 3. Temporal behavior of the measured emission signal (thick solid line) and reflectivity (thin solid line) of a silicon sample without antireflection (AR) coating, and the reflectivity of a sample with such a coating (dotted line).

propagation across this thin layer are of little significance because they appear only in the last 3 ps before the shock breakout.

In agreement with the absorption coefficient of cold silicon, the AR reflection signal in Fig. 3 (dotted curve) rises exponentially from the rest value of 0.07–0.1 to a maximum of  $R_{\lambda,\max} \approx 0.4$ . The fact that this value is close to the reflectivity of unperturbed and uncoated silicon should be considered as a mere coincidence. Because of the finite camera temporal resolution, the reflectivity of the shock front  $R_{\lambda,\text{sh}}$  may slightly exceed this value (by  $\approx 0.1$  according to our simulations). Hence, we use the value  $R_{\lambda,\text{sh}} = 0.4\text{--}0.05$  for the estimates below as the measured reflectivity of the 20.7 km/s shock front in silicon. It should be noted that we have no evidence of, but also no full control over, a possible contribution of the diffusive (nonspecular) component of the reflected probe-laser light outside the collection angle of the  $f/2$  imaging lens. However, such scattering could occur only on the shock front corrugated on a scale of the order of the laser wavelength.

The emission signal, measured for the shock speed  $D = 20.7 \pm 0.3$  km/s, peaked at  $F_{\lambda,\max} = 3.9 \pm 0.3$  W/cm<sup>2</sup> sr Å for  $\lambda = 532$  nm. Combining this value with the measured reflectivity of the shock front, we can apply Kirchhoff's law  $F_{\lambda} = (1 - R_{\lambda})B_{\lambda}(T_{\text{br}})$  (where  $B_{\lambda}$  is the Planckian intensity) to evaluate the brightness temperature  $T_{\text{br}} = 1.4 \pm 0.1$  eV of the emerging shock front. Note that this temperature is independent of any model for the opacity and transport and relaxation phenomena across the shock front. Confirming the earlier results by Celliers *et al.* [3,4], our value of  $T_{\text{br}}$  is considerably lower than the Hugoniot temperature either calculated with the present EOS (4.3 eV) or quoted in Ref. [4] for  $D = 20$  km/s ( $4.7 \pm 1.5$  eV).

The most natural cause of this discrepancy might be an extended relaxation zone across the shock front. To interpret our experimental results, we employed a 2- $T$  model based on the one-dimensional single-fluid hydrodynamic equations augmented with the Helmholtz equation for the electromagnetic waves as described in detail in Refs. [7,8]. Necessary ingredients for this model are the equation of state, the electron heat conduction and the  $e$ - $i$  temperature relaxation coefficients, and the dielectric permittivity at a given light frequency  $\omega$  (conductivity model). All of these processes are described within the theoretical model which has earlier proved to be adequate for interpretation of optical signals from the shock fronts in aluminum [7]. The pressure metallization of silicon within the density jump is described phenomenologically (but in a thermodynamically self-consistent manner) as an instantaneous increase in the equilibrium concentration of the free (conduction) electrons. Our calculated Hugoniot data for silicon agree well with those given in Ref. [4]. The conductivity model is constructed along the same lines as that by Lee and More [10] and in-

cludes the effects of Fermi degeneracy and strong ion-ion coupling.

Figure 4(a) shows the structure of a 20.7 km/s shock wave in silicon as calculated with our model. Because of the electron heat conduction, the electron temperature  $T_e$  is continuous across the jump of the ion temperature  $T_i$  and density  $\rho$ . The ionization degree jumps discontinuously from  $z \approx 1$  to  $z \approx 3$  because the band gap closes inside the density jump (at  $\rho = 3.6$  g/cm<sup>3</sup>). The critical density of free electrons (where the plasma frequency  $\omega_p$  is equal to  $\omega$ ) for  $\lambda = 2\pi c/\omega = 532$  nm occurs some 15 nm ahead of the density discontinuity in the electron precursor. The slope of the Poynting vector  $S_{\text{Poy}}$ , calculated by solving the Helmholtz wave equation for the  $\lambda = 532$  nm probe light and normalized to its value at 30 nm ahead of the density jump, illustrates the absorptivity (hence, the emissivity) of silicon across the shock front.

Calculated (without preheat) and measured optical signals are compared in Fig. 4(b). In order to fix the timing

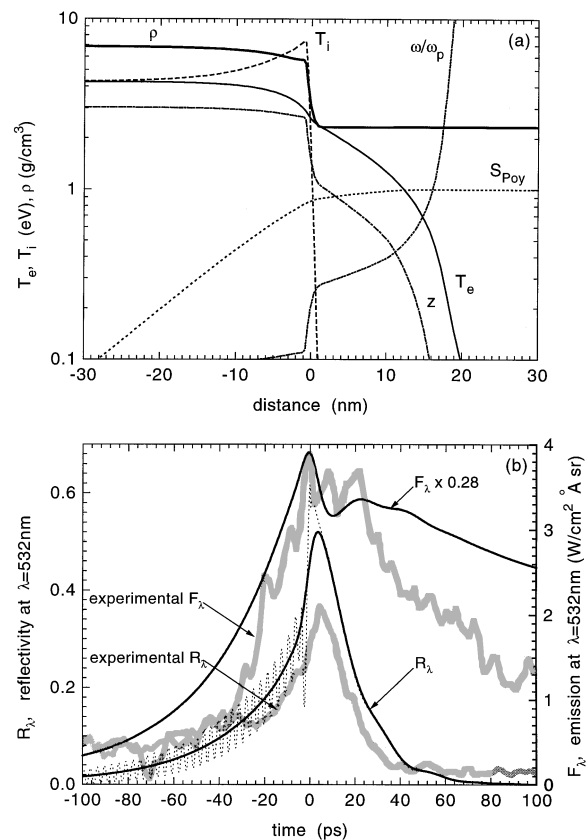


FIG. 4. (a) Structure of a 6.6 Mbar (20.7 km/s) shock wave in silicon. (b) Reflectivity  $R_{\lambda}$  (for the case with AR coating) and spectral emission  $F_{\lambda}$  (without AR coating) at  $\lambda = 532$  nm of a 20.7 km/s shock wave as calculated with our model (solid line). The calculated signals are smoothed with a 7 ps FWHM Gaussian distribution. Unsmoothed interference fringes (dotted line) are shown for the reflection signal only. The calculated  $F_{\lambda}$  curve has been multiplied by the indicated factor. The observed signals are plotted as thick grey lines.

between experiment and theory, the pair of experimental curves has been positioned for optimal overall agreement. Also, the intrinsic uncertainty (by about a factor of 2) of the conductivity model [7] was exploited to minimize the discrepancy with the experiment. As a result, a fair agreement between the theory and experiment was found for the reflectivity data  $R_\lambda$ , but not for the emission signal  $F_\lambda$ .

Similar to ordinary metals, our measured reflectivity  $R_{\lambda,sh}$  of the shock front provides direct information on the effective collision frequency  $\nu_{ei}$  of free electrons in the shocked state. Since all of the gradients across the shock front are steep compared to  $\lambda$ , we can apply the Fresnel formula together with the Drude model to evaluate  $\nu_{ei} = (5-15)\omega$  for  $R_{\lambda,sh} = 0.4-0.5$ ; here  $\omega = 2\pi c/\lambda = 3.54 \times 10^{15} \text{ s}^{-1}$ . This simple estimate for  $\nu_{ei}$  agrees well with the value  $\langle \nu_{ei} \rangle = 1.9 \times 10^{16} \text{ s}^{-1}$  calculated with our conductivity model in the hydrodynamic simulations. Note that, besides the shock reflectivity  $R_{\lambda,sh}$ , the collision frequency  $\nu_{ei}$  manifests itself in the decay slope of the  $R_\lambda$  curve after the shock breakout, and here also our experimental data agree with the above value of  $\nu_{ei}$ .

As is seen in Fig. 4(b), the measured peak of the shock emission  $F_\lambda$  (note the normalization factor for the theoretical curve) is about a factor of 3 lower than that predicted in the simulations. In terms of the peak brightness temperature, the 2- $T$  model predicts  $T_{br} = 3.45 \text{ eV}$  at  $\lambda = 532 \text{ nm}$ , while  $T_{br} = 1.4 \pm 0.1 \text{ eV}$  is actually observed. This discrepancy is significant and beyond the uncertainties of our conductivity model for the metallic state. Earlier, trying to explain a factor  $>10$  lower observed shock emission than that predicted by the equilibrium one-temperature model, Celliers *et al.* [3,4] assumed the  $e$ - $i$  temperature relaxation coefficient  $\chi_{ei}$  in silicon to be a free phenomenological parameter and obtained a best fit value of  $\chi_{ei} = 10^{16} \text{ W/m}^3 \text{ K}$ . In our model, within the logic of a self-consistent approach,  $\chi_{ei}$  is given in terms of the mean collision frequency  $\langle \nu_{ei} \rangle$  as  $\chi_{ei} = 3(m_e/m_i)n_e\langle \nu_{ei} \rangle$ , a relationship established for the Maxwellian and Fermi-Dirac electrons in the limit of weakly coupled plasmas [11]. For the collision frequency estimated above from the reflectivity data, we calculate a much higher value of  $\chi_{ei} \approx 6 \times 10^{18} \text{ W/m}^3 \text{ K}$ . If we simply decouple the  $e$ - $i$  temperature relaxation from the conductivity model and perform a simulation with a fixed value of  $\chi_{ei} = 10^{16} \text{ W/m}^3 \text{ K}$ , we do indeed calculate a peak value of the emission close to what is observed, but find significant discrepancies with its measured temporal profile.

In conclusion, for the first time our advanced experiments with x-ray driven shock waves of controlled, very low preheat have, through simultaneous reflection and emission measurements, established a complete data set

and, in particular, a model-independent brightness temperature which can now serve as a touchstone for theory. It turns out that the present nonequilibrium 2- $T$  models do not provide an adequate framework for interpretation, suitable to bridge the gap to the Hugoniot temperature. Which processes precisely require a more detailed description, is not clear at the moment. A major flaw may have to do with the kinetics of the dielectric-metal phase transition, if the latter extends over a layer comparable in thickness to the skin depth. Also, the one-dimensional modeling might be inappropriate if the shock front is not perfectly smooth on a 10–100 nm scale. And although, because of the high quality of the x-ray drive and sample surfaces, we do not see any reason for shock corrugations, there has been no experimental information to this point so far.

We express our gratitude to S.I. Anisimov for many stimulating discussions, and thank K. J. Witte for a critical reading of the manuscript.

---

\*On leave from Troitsk Institute for Innovation and Fusion Research, Troitsk 142092, Moscow Region, Russia.

†On leave from Institute for Theoretical and Experimental Physics, Moscow 117259, Russia.

‡On leave from Max-Planck-Institut für Quantenoptik, D-85748 Garching, Germany; Technische Hochschule Darmstadt, Germany.

- [1] Ya.B. Zel'dovich and Yu.P. Raizer, *Physics of Shock Waves and High Temperature Hydrodynamic Phenomena* (Academic, New York, 1966); Chap. XI.
- [2] Ya.B. Zel'dovich, S.B. Korner, and V.D. Urlin, *Zh. Eksp. Teor. Fiz.* **55**, 1631 (1968) [*Sov. Phys. JETP* **28**, 855 (1969)].
- [3] P. Celliers, A. Ng, G. Xu, and A. Forsman, *Phys. Rev. Lett.* **68**, 2305 (1992).
- [4] A. Ng, P. Celliers, G. Xu, and A. Forsman, *Phys. Rev. E* **52**, 4299 (1995).
- [5] S. Minomura and H. G. Drickamer, *J. Phys. Chem. Solids* **23**, 451 (1962).
- [6] Th. Löwer, R. Sigel, K. Eidmann, I.B. Földes, S. Hüller, J. Massen, G.D. Tsakiris, S. Witkowski, W. Preuss, H. Nishimura, H. Shigara, Y. Kato, S. Nakai, and T. Endo *Phys. Rev. Lett.* **72**, 3186 (1994).
- [7] M. Basko, Th. Löwer, V.N. Kondrashov, A. Kendl, R. Sigel, and J. Meyer-ter-Vehn, *Phys. Rev. E* **56**, 1019 (1997).
- [8] P. Celliers and A. Ng, *Phys. Rev. E* **47**, 3547 (1993).
- [9] H.A. Weakliem and D. Redfield, *J. Appl. Phys.* **50**, 1491 (1979).
- [10] Y. T. Lee and R. M. More, *Phys. Fluids* **27**, 1273 (1984).
- [11] H. Brysk, *Plasma Phys.* **16**, 927 (1974).